Topological effects in ring polymers: A computer simulation study

M. Müller,* J. P. Wittmer,† and M. E. Cates
Deptartment of Physics & Astronomy, University of Edinburgh, King's Building, Mayfield Road, Edinburgh EH9 3JZ, United Kingdom
(Received 18 September 1995)

Unconcatenated, unknotted polymer rings in the melt are subject to strong interactions with neighboring chains due to the presence of topological constraints. We study this by computer simulation using the bond-fluctuation algorithm for chains with up to $N=512$ statistical segments at a volume fraction $\Phi=0.5$ and show that rings in the melt are more compact than Gaussian chains. A careful finite-size analysis of the average ring size $R \propto N^{\nu}$ yields an exponent $\nu \approx 0.39 \pm 0.03$ in agreement with a Flory-like argument for the topological interactions. We show (using the same algorithm) that the dynamics of molten rings is similar to that of linear chains of the same mass, confirming recent experimental findings. The diffusion constant varies effectively as $D_N \propto N^{-1.22(3)}$ and is slightly *higher* than that of corresponding linear chains. For the ring sizes considered (up to 256 statistical segments) we find only one characteristic time scale $\tau_{ee} \propto N^{2.0(2)}$; this is shown by the collapse of several mean-square displacements and correlation functions onto corresponding master curves. Because of the shrunken state of the chain, this scaling is *not* compatible with simple Rouse motion. It applies for all sizes of ring studied and no sign of a crossover to any entangled regime is found.

PACS number(s): 61.25.Hq, 61.41.+e

I. INTRODUCTION

Ring polymers have been extensively studied experimentally by several groups, not always leading to completely consistent results [1–7]. Indeed, the synthesis of the samples of unknotted and nonconcatenated rings (see Fig. 1) remains a very delicate issue [5]. Nevertheless, the general conclusion emerging from these studies is that the dynamics of rings is quite similar to that of linear chains of the same molecular mass and density [8,7]. This is certainly a surprising result from the point of view of the reptation model, which describes the flow behavior of entangled linear polymer chains [9,10]. In this effectively single-chain model, the constraints on the motion of a reference chain due to the interactions with its neighbors are replaced by a curvilinear ''tube'' within which the chain ''reptates:'' relaxation of the constraints occurs only at the chain ends. Clearly, a closed ring polymer (having no ends) cannot reptate in this conventional sense. Accordingly, the motion in a melt of rings should be quite different from that of an analogous linear chain system and at first sight one would expect it to be slower. Indeed it was argued [11,10] that motion of ring polymers should be exponentially slow and comparable with that of star polymers [12].

This is, however, not borne out by rheological measurements on polystyrene (PS) and polybutadyene (PB) rings, which showed that the zero-shear viscosities η_0 for melts of rings for all molecular weights considered are similar to, but even slightly smaller than, those for linear chains [2,5]. The temperature dependence of η_0 in PS rings is virtually indistinguishable from that of linear polystyrene of high enough molecular weight; all viscosities display classical Williams-Landel-Ferry (WLF) or Vogel-type temperature dependence and they can be superimposed on a single master curve. For linear chains, two power-law regimes arise in the mass dependence of the viscosity, corresponding to Rouse-like and entangled motion. Unexpectedly, the same is found for ring polymers. Below a critical mass M_c the viscosity seems to increase with an exponent $\alpha_1 \approx 3/2$, which is larger than the expected $\alpha_1=1$ for ideal Rouse behavior. The values for rings and linear chains of the same molecular weight are of similar magnitude. In the high mass regime ($M>M_c$) the viscosities increase more strongly, again with a power similar to the linear case. An exponential increase in the range of

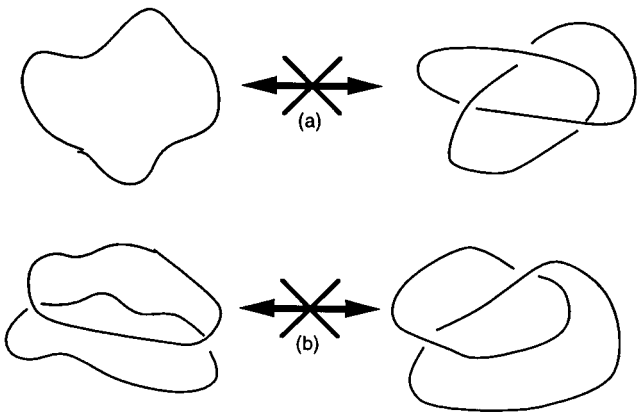

FIG. 1. Sketch of the opposed topological constraints. (a) On the left is a permitted configuration of an unknotted ring. It cannot turn into the forbidden (knotted) configuration on the right (nor vice versa). (b) On the left is a permitted configuration of a pair of unknotted, unconcatenated rings. It cannot turn into the forbidden (concatenated) configuration on the right (nor vice versa).

*Permanent address: Institut für Physik, Johannes-Gutenberg Universität, 55099 Mainz, Germany.

†Author to whom correspondence should be addressed. Permanent address: Cavendish Laboratory, Madingley Road, Cambridge CB3 0HE, United Kingdom.

masses available (up to $M \approx 1.85 \times 10^5$) is explicitly excluded [5,13].

The similarity of the dynamics of ring molecules to their linear counterparts is also reported on a more microscopic level from tracer diffusion measurements [6,7]. Dilute labeled PS chains of mass M, in a matrix of mass P, were measured using forward recoil spectroscopy. Different topologies (rings in linear matrices [6], linear chains in ring matrices [7], and rings in microgel [7]) were investigated and compared to linear chains in linear matrices. Unfortunately, there exist so far no systematic measurements of ring tracers in matrices of rings (of identical size) in which the molecular mass covers a significant range. However, consistent with the rheological measurements quoted above, the tracer diffusion of linear PS in ring matrices was found to be nearly identical to that of linear PS in linear PS matrices [7,14]. This is again a surprising result in view of theoretical concepts of matrix-dependent tracer diffusion [11].

A suggestion by Lodge *et al.* [10] is that the experiments on rings may be reconciled with the reptation concept by taking into account the higher entanglement length. The critical mass for entanglement can be estimated from the viscosities or from the shear modulus. PS rings exhibit a plateau modulus approximately one-half (one-fifth for PB) that for linear polymers, suggesting that rings are less effective at forming entanglements. Rubber elasticity arguments indicate a critical mass for polystyrene cycles of $M_c = 58\,000$ compared to $M_c = 30\,000$ for linear chains. If one now makes a comparison *at an equal number of entanglements* ring melts in fact have higher viscosities than linear chains. The experimental viscosity data then lie in the unentangled-entangled crossover region, where it is clear from the linear polymer results that reptation is not the only available mode. This explanation would allow a crossover to much slower ring dynamics at very high molecular weights.

No theoretical explanation for this increase of the critical mass exists, but it seems reasonable to relate it to the idea that ring conformations in the melt may be partially collapsed [15]. Besides the usual excluded volume interaction between two neighboring chains there is a topological interaction due to the exclusion of knotted and concatenated ring configurations (see Fig. 1). While the excluded volume interaction is screened out whenever the overlap with other chains is large (i.e., as long as $R^d/N \gg 1$, which is true for large chains if $\nu > 1/d$) the topological interaction in three-dimensions need not be screened and should cause a reduction in the size exponent ν below the Gaussian value ($\nu = 1/2$).

Despite this argument, no experimental study of the radius of gyration of rings in the melt appears to have been made. A good understanding of the static properties of the system is of course an indispensable starting point for a reasonable description of the dynamics, so this is unfortunate. Detailed static measurements (in both dilute and concentrated systems) could also provide a stringent test on the quality of the ring synthesis, as McKenna *et al.* have pointed out [8]. Without them, for many synthesis routes it is hard to exclude the possibility of knotted or concatenated rings, along with that of a small fraction of linear chain contaminants, which might modify the viscosity substantially (by threading the rings, for example) [5].

In view of those experimental difficulties, a detailed simulation study to investigate both the statics and the dynamics in a melt of rings is certainly warranted. Most previous attempts are based on Pakula's ''cooperative motion algorithm'' [16,17]. While this algorithm can give correct results for the statics (especially for melts), its value for studying dynamics is questionable (see Sec. II below). In the following we study melts of nonknotted, nonconcatenated rings within the well-established ''bond-fluctuation model'' (BFM) to get better insight in their statics and dynamics. Apart from its computational efficiency, an advantage of the method is that comprehensive data for linear chains have already been obtained [18,19] with which quantitative comparisons can be made. Indeed, even if ring polymers did not exist experimentally, this comparison might help illuminate several long-standing but still controversial issues in the dynamics of entangled linear chains [20].

The article is organized as follows. In Sec. II we give briefly some technical comments on the BFM simulation performed. In Sec. III results on the conformation of isolated rings (in an athermal solvent) are presented, showing that the unknottedness constraint is insufficient to swell the rings significantly beyond what would be caused by excluded volume forces alone. Molten rings, on the other hand, are found to be quite compact with an exponent $\nu \approx 0.4$, consistent with the assumption [15] that roughly one degree of freedom is lost for every topological interaction with a neighboring chain. We then show, in Sec. IV, that the dynamics of rings and linear chains are qualitatively similar over much of the range of chain length that we are able to simulate. For the largest rings, however, a perfect scaling (involving a single characteristic time for each chain length) is still obeyed, whereas for this size of linear chain significant departures are observed. This allows us to confirm the suggestion that the entanglement mass is much larger for rings.

We also study the degree to which rings thread through one another, a question addressed in both Secs. III and IV. This seems to be insufficient to allow large clusters of mutually entangled material to build up. The extent of entanglement, quantified roughly as the number of neighboring rings contacting a given molecule, nevertheless appears relevant for dynamics: for both rings and their linear counterparts the diffusion constant is shown to scale as the mass of the correlation hole (at least, in the range of chain lengths studied). Finally, in Sec. V we give our conclusions and discuss the impact of these ring investigations on our understanding of entangled polymer dynamics.

II. A BOND-FLUCTUATION MODEL STUDY

The algorithm used in this investigation is the well-established bond-fluctuation model of Carmesin and Kremer [21]. This coarse-grained three-dimensional lattice model has proven to be especially useful for investigating the universal features of statics and dynamics in dense polymeric melts [18]. A small number of chemical repeat units (i.e., a Kuhnian segment) is mapped onto a lattice monomer such that the relevant characteristics of polymers are retained: connectivity of the monomers along a chain and excluded volume of the monomers. Each monomer occupies a whole unit cell of a simple cubic lattice with periodic boundary conditions.

Adjacent monomers along a polymer are connected via one of 108 allowed bond vectors. These are chosen such that the local excluded volume interactions prevent the chains from crossing each other during their motion. This conservation of the topology ensures that the rings (which are set up initially as thin loops) remain neither knotted with themselves nor concatenated with one another during the relaxation and sampling. In our athermal simulation, ''local jumps'' are realized by choosing one monomer at random and attempting to jump over the distance of one lattice spacing in one of the six basic directions (also randomly chosen). The attempt is accepted if excluded volume restrictions are satisfied and the new bond vectors to the neighbors along the ring belong to the allowed set.

A simulation study of ring polymers has already been made by Frisch *et al.* [22] in the framework of the BFM. However, due to the large CPU time demands, that study was restricted to single rings; also the dynamical properties were not very directly addressed. The only existing simulation data on the statics and dynamics of rings in the melt use Pakula's ''cooperative rearrangement algorithm'' [23,24]. In contrast to the local jumps utilized in the BFM, this algorithm changes simultaneously and collectively the monomer positions on a number of different chains. While giving correctly the static properties, a clear correspondence between Monte Carlo time and real time is yet to be established for this algorithm and its dynamical interpretation is accordingly unclear.

In the present BFM investigation we want to extend the careful study of linear chains made by Paul *et al.* [18] to ring polymers and compare our results to their data on linear chains. At a filling fraction $\Phi=0.5$ of occupied lattice sites, many static and dynamic features of molten polymeric materials are reproduced by the BFM. For example, the single-chain conformations obey Gaussian statistics down to the screening length $\xi\approx 6$ (in units of the lattice constant) of the excluded volume interaction obtained from the static structure factor [18]. There are extensive results on the dynamical properties covering the range from an unentangled behavior for short chain lengths up to the onset of reptationlike motion for chain length $N=200$. Of course, the dynamics of long polymers in a dense melt slows down dramatically with growing chain length and therefore poses huge demands on CPU time requirements. For the present investigation we employ a very efficient implementation of the BFM on a massively parallel CRAY T3D supercomputer [25]. Using a two-dimensional geometrical decomposition of the simulation grid of linear extension $L=128$, we employ 64 T3D processors. This permits us to equilibrate systems comprising 131 072 monomers and ring lengths up to 512 (statics) or 256 (dynamics) statistical segments. This study involved about 5000 h of single processor CPU time.

The starting configurations consisted of straight rings (loops enclosing no area) that were carefully equilibrated for at least one relaxation time (i.e., the center of mass had moved a distance comparable to the chain size) before any data were taken. Indeed, for all but the longest chains, runs were continued well beyond this (so as to generate dynamical data), which enabled us to confirm that the static chain extensions had settled to their equilibrium values by this time.

TABLE I. Mean-square bond length $\langle b^2\rangle$, radius of gyration $\langle R_g^2\rangle$, ring diameter $\langle R_e^2\rangle$, and diffusion constant D_N for single unknotted rings.

N	$\langle b^2\rangle$	$\langle R_g^2\rangle$	$\langle R_e^2\rangle$	D_N (units of 10^{-4})
16	7.436	17.5	59.9	20.5(20)
32	7.455	41.1	140.2	12(2)
64	7.464	95.9	322.9	5.2(4)
128	7.468	221.9	739.6	2.55(20)
256	7.470	510	1698	1.25(20)
512	7.472	1159	3740	0.72(10)

III. STATICS: CONFORMATIONS OF RINGS IN THE MELT

In this section we consider the effects of the unknottedness and nonconcatenation constraints on the conformational properties of dilute and molten rings. While the effect of the former constraint on isolated rings turns out to be irrelevant, the nonconcatenation requirement significantly compacts molten rings.

The size of the rings is measured first with the usual mean-square radius of gyration $\langle R_g^2\rangle$; as a second measure, we define the average distance between pairs of monomers that are $N/2$ monomers apart along the ring contour $\langle R_e^2\rangle=\langle(\vec{R}_n-\vec{R}_{n+N/2})^2\rangle$ and call this the mean-square ring diameter. For isolated rings in an athermal solvent, results for both quantities are presented in Table I. In agreement with previous Monte Carlo studies by Frisch *et al.* [22], the simulation yields a ring size $R\propto N^{\nu}$ with exponent $\nu\approx 0.595$ for the radius of gyration and $\nu\approx 0.605$ for the ring diameter. These values are only slightly larger than the excluded volume exponent ($\nu=0.588$) for linear athermal chains, the difference lying within the range of the statistical error. The influence of the topological constraints on the static properties of isolated rings thus appears not to alter the chain-swelling exponent in three dimensions (though there may be a prefactor effect) [26]. This finding concurs with the analytical studies of des Cloizeaux and Metha [27] and is now also confirmed experimentally. Indeed, while early small-angle neutron-scattering data of Dogson and Higgins [1] seemed to indicate a nearly Gaussian statistics for rings in good solvent, later the delicate dependence of the ring properties on preparation conditions was overcome by Hadziioannou [3] and Roovers [2] corroborating that the statistics are the same as for linear chains in a good solvent. However, a decrease of the θ temperature of isolated rings (compared to linear chains) by several degrees kelvin has been measured. This is defined by the point at which the second virial coefficient from the light scattering measurements equals zero and seems to be the only manifestation of the unknottedness constraint [2,5]. A Monte Carlo study of the θ-point depression of isolated rings, including a careful finite-size analysis, could certainly yield interesting additional information; we do not attempt this here.

The situation changes completely in the other limit of molten rings where, confirming Pakula's simulation [16], we find very compact rings (Table II). When naively fitted without any finite-size analysis, the ring sizes yield an exponent $\nu\approx 0.44$ for the ring diameter R_e and a slightly higher value

TABLE II. Mean-square bond length $\langle b^2 \rangle$, radius of gyration $\langle R_g^2 \rangle$, ring diameter $\langle R_e^2 \rangle$, ring surface A, number of neighbors touching a reference chain n_N, monomer mobility W, diffusion constant D_N, and rotational relaxation time τ_{ee} for unknotted, unconcatenated rings in the melt at volume fraction $\Phi = 0.5$.

N	$\langle b^2 \rangle$	$\langle R_g^2 \rangle$	$\langle R_e^2 \rangle$	A	n_N	W (units of 10^{-3})	D_N (units of 10^{-4})	τ_{ee} (units of 10^{+4})
16	6.904	12.9	42.3	12.36	10.88	5.2	3.67(25)	0.58
32	6.913	25.7	80.6	23.30	13.60	6.6	1.62(21)	2.2
64	6.920	49.3	150.3	42.46	17.01	7.3	0.66(12)	8.7
128	6.924	92.2	274.8	76.66	21.15	7.5	0.285(45)	35
256	6.926	169.7	497.2	135.36	26.18	6.6	0.126(21)	160
512	6.927	304.0	878.0	229.88	31.50			

$\nu \approx 0.45$ for the radius of gyration R_g. Those values are quite similar to the ones obtained by Pakula. However, finite-size corrections are clearly detactable in the curvature of the data points and a more careful fitting is necessary, as explained below and in Fig. 2. This yields in an extrapolation to the limit of infinite masses a distinctly lower exponent $\nu = 0.39 \pm 0.03$, which (as it should) becomes the same for our two measures of ring size R_e and R_g.

At the volume fraction $\Phi = 0.5$ used in the simulation, the excluded volume interaction is not completely screened, as pointed out in Sec. II. This explains why the radius of gyration, which is more sensitive to short-scale structure, tends to give larger exponents $\nu(N)$ than the diameter that probes larger distances (Fig. 2). At high masses this short-scale effect of the excluded volume will become less and less important, so both the ratio of diameter to the radius of gyration (inset of Fig. 2) and the running exponents $\nu(N)$ tend to become smaller. These exponents are plotted against the natural variable of the screening (proportional to ξ/R_g) [30]; the procedure brings all the measured values $\nu(N)$ to lie on straight lines, which permit a precise finite-size scaling analysis [31]. As one sees from Fig. 2, the low masses give exponents close to those obtained previously; the highest masses used yield an exponent $\nu \approx 0.42$. Only in the limit of infinite masses does the short-scale excluded volume effect vanish and the two lines for R_e and R_g merge at a value $\nu = 0.39 \pm 0.03$.

This value is consistent with a crude but interesting Flory-like estimate of the free energy of a polymer ring given by Cates and Deutsch [15]. They argued that, if a ring of polymerization index N has size R, it is overlapped with a number of neighboring rings of order R^d/N (in d dimensions). The more spatially extended the ring, the more entropy is lost by the nonconcatenation constraint with its neighbors. The simplest possible estimate of this is to say that the number of degrees of freedom lost due to the constraint is proportional to the number R^d/N of neighbors that the ring is prevented from threading. This gives a contribution to the free energy of $F \propto kTR^d/N$ tending to decrease the ring size. On the other hand, there is also an entropy penalty if the ring becomes too squashed; the free energy required to squash a Gaussian chain of N steps into a region of linear size R less than $N^{1/2}$ scales as kTN/R^2. Adding these contributions and minimizing over R gives a characteristic size scaling as $R \propto N^{\nu}$ with $\nu = 2/(d+2)$. Hence, in three dimensions the exponent is $\nu = 2/5$, very close to the value found by our simulation. Note that the latter value is definitely smaller than the result $\nu = 1/2 - 1/6\pi$ put forth recently by Brereton and Vilgis [32].

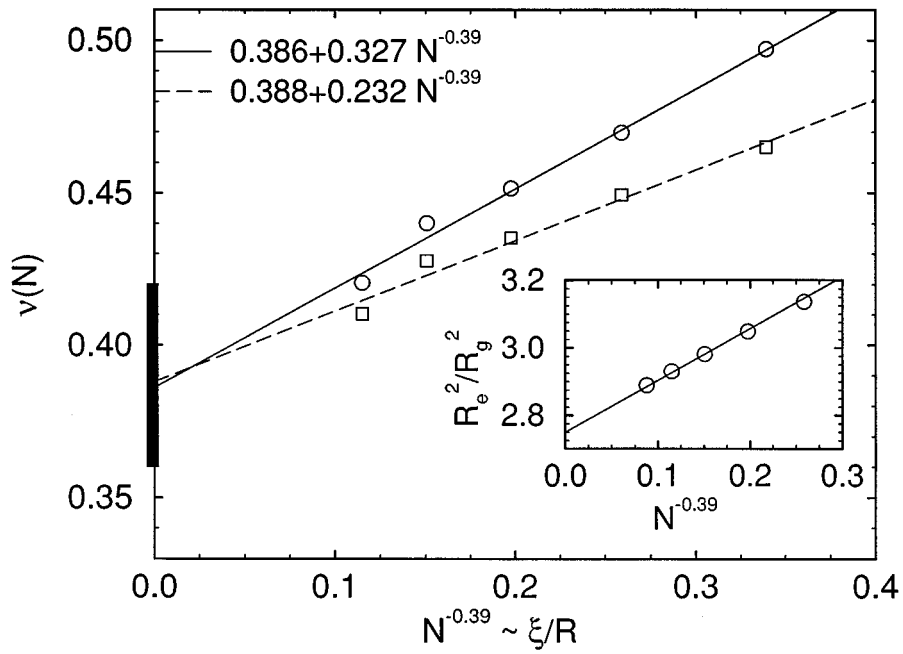

FIG. 2. Running exponents $\nu(N)$ obtained from the radius of gyration $\langle R_g^2 \rangle$ (circles) and the ring diameter $\langle R_e^2 \rangle$ (squares) versus the natural variable of the screening $N^{-\nu}$. Both the two exponents and the ratio $\langle R_e^2 \rangle / \langle R_g^2 \rangle$ in the inset lay on straight lines. From this finite-size analysis we obtain the exponent $\nu \approx 0.39 \pm 0.03$ in the limit of infinite mass.

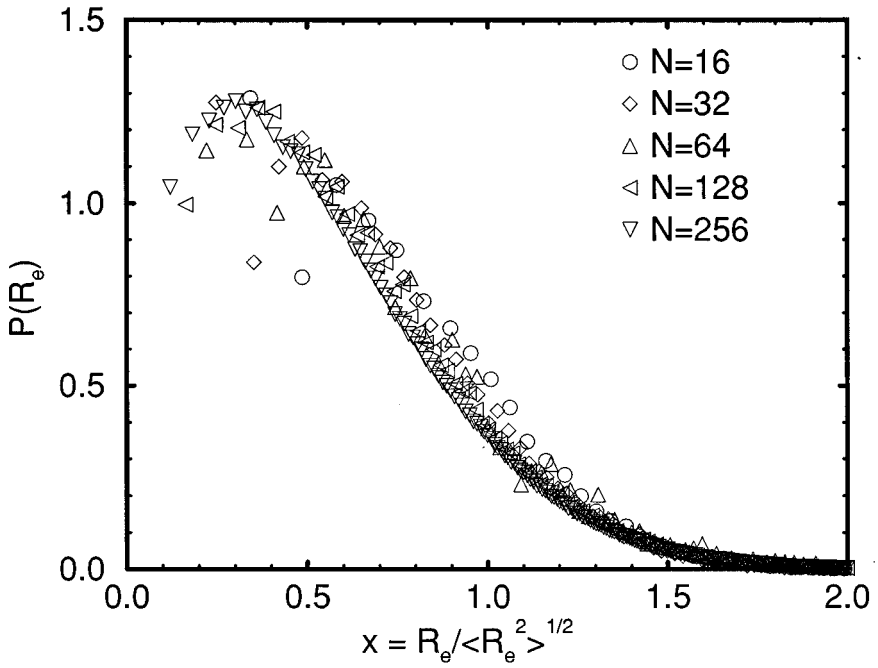

FIG. 3. Distribution function of the ring diameter R_e as a function of the reduced variable $R_e/\langle R_e^2\rangle^{1/2}$. Data for various masses are distinguished by different symbols, as indicated in the figure. Apart from the very small chains, all distributions superimpose.

We note that from the measured exponents of the chain size of an isolated chain $\nu_0 \approx 0.6$ and of ring chains $\nu_m \approx 0.4$ a crossover scaling can be obtained in the usual way. This yields, for the ring size in the semidilute concentration range, $R \approx R_0(\Phi/\Phi^*)^{-1/4}$, where the monomer density is Φ and the usual crossover density (overlap threshold) is Φ^*. The decrease in the size of a ring with Φ is much more pronounced than for linear chains where $R \sim \Phi^{-1/8}$.

In Fig. 3 we show simulation data for the probability distribution $P(R_e)$ of the diameter of a ring as a function of the characteristic variable $x = R_e/\langle R_e^2\rangle^{1/2}$. Data are given for various masses up to $N = 256$. The scaling collapse becomes more and more perfect with increasing mass, indicating again that the local interactions become irrelevant for ring sizes much larger than the excluded volume screening length ξ. In principle, this distribution should define some further characteristic exponents, assuming that, as for linear chains [33], the distribution rises with a power $P(x) \propto x^g$ for small x and drops off essentially as $P(x) \propto x^a \exp(-x^\delta)$ for large x. For isolated linear chains the exponents g and δ can be written in terms of ν and γ (the latter is the exponent controlling the N dependence of the free energy). Unfortunately, although the scaling in Fig. 3 is good, the data are not precise enough to extract any corresponding exponents in this case. Accordingly, we leave this issue for future investigations.

A quantity of more direct experimental relevance than $P(r)$ is the static structure factor $S(q)$. In Fig. 4 the values of $S(q)/N$ for masses up to $N = 512$, expressed as a function of the characteristic variable $R_g q$, superimpose (apart from the spurious Bragg peak in each case) onto a single master curve. Consistent with our earlier discussion of the scaling of the ring size, a self-similar power-law regime is apparent and shows a fractal dimension $1/\nu = 1/0.4$, as expected. The Gaussian dimension 2 is clearly ruled out by our data [34].

As mentioned in the Introduction and above, the probability of threading of a ring polymer by its neighbors is implicated in the mechanism of partial collapse and may also have dynamical consequences by way of long-lived clusters of entangled material slowing down the relaxation times. It is difficult to define precisely what is meant by threading (in either static or dynamical terms), but a partial measure of the ease with which a ring can be threaded is to measure the area of its projection onto a random direction. This area a is defined as a signed quantity (the component in that direction of the vector area of the ring) that vanishes for any configuration in which the ring exactly retraces its own steps. A measure of the ''threadability'' is provided by $A = \langle |a| \rangle$; it turns out that $A \propto R_g^2$, as shown in Fig. 5. The scaling is the same as would be naively expected. Note that looplike configurations would involve very small values of A. The magnitude $A/R_g^2 \approx 1$ indicates that the rings have no tendency to retrace their own steps, a fact also revealed by inspection of snapshots.

Another quantity that may be relevant in measuring the strength of the topological interactions is the number of chains touching a reference chain n_N. Two chains are defined to be ''touching'' whenever their monomers include pairs separated by a distance less than or equal to $\sqrt{6}$ lattice constants. (This somewhat arbitrary microscopic distance was chosen to include all the monomers within the first peak of the monomer-monomer correlation function.) Intuitively, n_N should vary as the number of chains within the ''correlation hole'' spanned by a given chain, and we see in Fig. 5 that n_N indeed scales as R_g^3/N. The plateau at high enough masses confirms the self-similarity of rings in the melt, which was already indicated by the scale invariance of the diameter distribution in Fig. 3.

IV. DYNAMICS OF RINGS IN THE MELT

As pointed out in the Introduction, there is some experimental evidence that the dynamics of rings are similar to

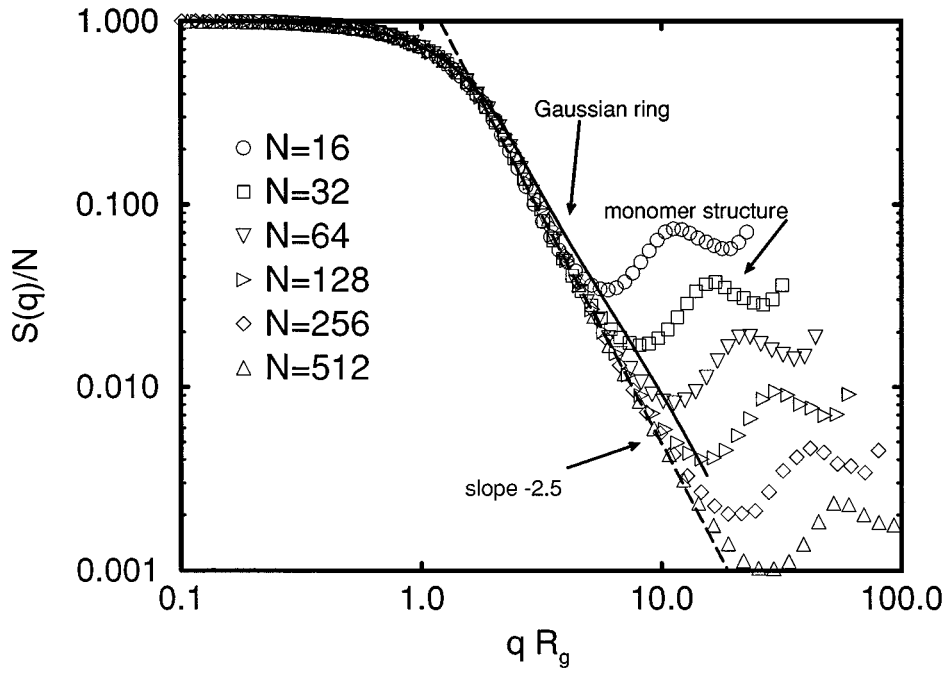

FIG. 4. Structure factor $S(q)/N$ versus the characteristic variable $R_g q$ for various masses N as indicated in the figure. The dashed line confirms the fractal dimension $1/\nu = 2.5 = 1/0.4$. The solid slope 2 for rings with Gaussian statistics cannot match the measured structure factor.

their linear counterparts, at least up to the largest molecular masses that can readily be obtained. Our simulation data, presented below, confirms this for rings of up to $N=256$ monomers by comparing mean-square displacements, chain and cooperative motion correlation functions, and the resulting diffusion coefficients and relaxation times.

We characterize the dynamics by measuring three different mean-square displacement functions describing the motion of monomers $g_1(t)=\langle[\mathbf{R}_n(t)-\mathbf{R}_n(0)]^2\rangle$ in the laboratory frame, the motion of monomers in the center-of-mass frame of a given ring $g_2(t)=\langle[\mathbf{R}_n(t)-\mathbf{R}_{\text{c.m.}}(t)-\mathbf{R}_n(0)+\mathbf{R}_{\text{c.m.}}(0)]^2\rangle/2$, and the motion of the center of mass itself $g_3(t)=\langle[\mathbf{R}_{\text{c.m.}}(t)-\mathbf{R}_{\text{c.m.}}(0)]^2\rangle$. The mean-square displacement functions for molten rings are given in Fig. 6. These quantities are scaled by the mean-square characteristic ring size $\langle R_g^2\rangle$, whereas the time coordinate is scaled by the rotational relaxation time τ_{ee}. This rotational time is the decay time for relaxation of a ring diameter (the vectorial displacement between monomers $N/2$ apart in the sequence), which is obtained from the correlation function $C_{ee}(t)$ described below (shown in Fig. 10), and its scaling with N is shown in Fig. 11. Apart from the mass $N=16$ all curves perfectly superimpose with the use of this single scale factor for each chain. This indicates that no second time scale is present as

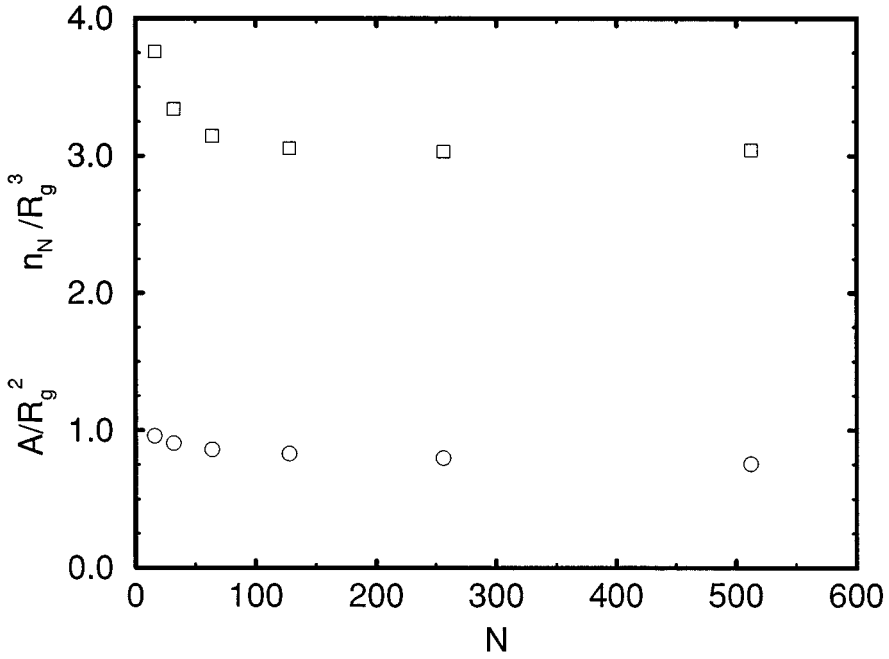

FIG. 5. Surface circumscribed by a ring in the melt A, plotted as A/R_g^2 (circles), and the number of neighbors n_N, plotted as $n_N N/R_g^3$ (squares) versus N. The mass-independent plateaus 0.8 and 3, respectively, are reached for masses larger than $N=100$.

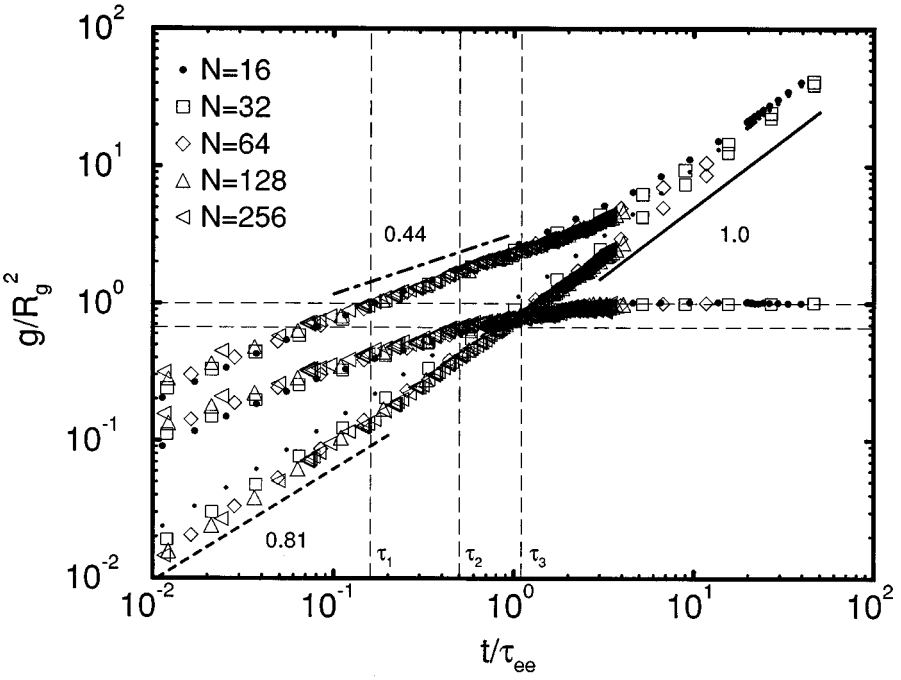

FIG. 6. Mean-square displacements of a ring monomer $g_1(t)$, of a monomer in the frame of the center of mass $g_2(t)$ and of the center of mass $g_3(t)$ versus the reduced time t/τ_{ee}. The three times $\tau_{1,2,3}$ (vertical dashed lines) are defined in the text. The two horizontal dashed lines correspond to mean-square displacements of $2/3\langle R_g^2\rangle$ and $\langle R_g^2\rangle$, respectively. The Fickian behavior at long times is indicated by the solid line. The effective exponent $x=0.81$ of the center of mass motion at shorter times due to net forces of neighboring chains is displayed by the broken line. The anomalous diffusion of a monomer for molten rings with exponent $\nu=0.4$ is indicated by the dash-dotted line.

would be expected for an entangled system (the entanglement time). Such scaling is sometimes called Rouse behavior [18], but here we describe it as ''unentangled scaling'' since the power laws involved need not be those of the Rouse model. Notably, no crossover whatsoever is detectable from this scaling to a modified (reptation or other) motion, involving a second time scale, even for the largest rings studied ($N=256$). This contrasts with the fact that for linear chains of mass larger than $N=200$ the unentangled scaling starts to break down, with clear signs of a crossover to a new regime (whose exponents could not, however, be reliably measured) [19]. This finding confirms that any entanglement length for rings is larger than that for linear chains of the same type, in agreement with experimental inference [4,8].

As mentioned before, it is tempting to associate this with the fact that the rings are partially collapsed. Crudely, one could argue that for a given degree of entanglement, the number of chains in the correlation hole (which scales as R_g^3/N) should be the same for rings and linear chains. This would give a rough estimate of $N=1000$ BFM monomers as the breakdown point of the unentangled scaling in the ring case. This estimate is broadly consistent with the entanglement mass for rings reported in experiments as lying between 2 (for PS) or 5 (for PB) times as large as for linear chains, as discussed in the Introduction.

Qualitatively, the mean-square displacements of rings displayed here show behavior very similar to that of short linear chains, up to masses of order $N=100$ [18,19]. (However, as mentioned above, for larger masses the scaling breaks down in the linear chain case, and in this regime the rings and linear chains are no longer precisely alike.) While the center of mass follows the Fickian type of diffusion at long times ($t/\tau_{ee}\gg 1$), a clear signature of net forces acting on the center of mass of the chains is displayed at short times, when the center-of-mass displacement g_3 is proportional to $(t/\tau_{ee})^x$, with an effective exponent $x\approx 0.81$. (Within a true Rouse model, in which each monomer in the system is subject to uncorrelated random forces, this exponent would have the Fickian value of unity at all times.) This effect was also observed for linear chains with a slightly higher effective exponent $x\approx 0.85$ at the same density $\Phi=0.5$ [18,19]. There it was also verified that the exponent x is density dependent, approaching 1 in the low density limit; it is very likely that this is similar for rings. We can therefore conclude that, as for linear chains, there is a net force acting on the center of mass generated by the interaction of the test chain with surrounding ones, slowing down the chain motion at short times.

The monomer motion may also be split into two regimes characteristic of short and long times. While in the latter the monomeric displacements approach asymptotically that of the whole chain [$g_1(t)\propto t$], the conformational properties of the rings in the melt are reflected in the short-time anomalous diffusion regime. The involvement of more and more ring monomers as the lifetime of a fluctuation increases gives by general scaling arguments a mean-square monomer displacement of $g_1\propto(t/\tau_{ee})^{1/(1+1/2\nu)}$. For our rings ($\nu\approx 0.4$) this yields an exponent of about 0.45, which agrees well with the dynamical simulation data shown in Fig. 6. [The agreement is even better if one uses for each chain length the measured exponent $\nu(N)$, which is somewhat larger than the extrapolated value $\nu(\infty)$, as explained in Sec. III.] Defining a monomeric mobility W by $g_1=b^2(Wt)^{1/(1+1/2\nu)}$, where b is the monomer size, perhaps surprisingly we find (as shown in Table II) that $W\approx 7\times 10^{-3}$ for rings is about 4 times larger than for linear chains, where $W\approx 1.6\times 10^{-3}$. The mean-square monomer displacement in the frame of the center of mass g_2 follows (as expected), for small times, the same behavior as that in the laboratory frame g_1, while for long times it approaches (by definition) the mean-square radius of gyration of the rings.

In order to characterize succinctly the mean-square displacement curves for rings and to compare them with the linear chain counterparts, we define (following Ref. [18])

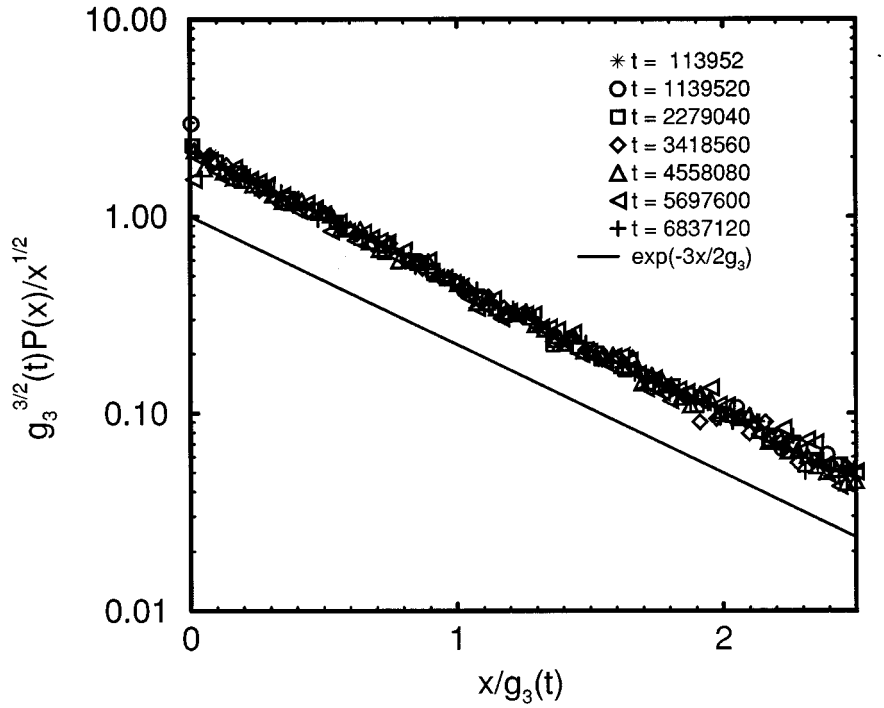

FIG. 7. Distribution $P(x)$ of the mean-square displacements x of the center of mass $g_3(t)$ for chains of mass $N=256$. Data over a large range of time (as indicated in the figure) collapse perfectly on one straight line with slope $-3/2$ when plotted as $g_3^{3/2}(t)P(x)/x^{1/2}$ versus $x/g_3(t)$, corresponding to a Gaussian distribution of the displacement variable.

three characteristic times $\tau_{1,2,3}$ according to the following criteria: $g_1(\tau_1)=\langle R_g^2\rangle$, $g_2(\tau_2)=2/3\langle R_g^2\rangle$, and $g_2(\tau_3)=g_3(\tau_3)$. Each τ parameter is a measure of the decay of the corresponding displacement function, as indicated in Fig. 6. Apart from a bit of scatter we obtain, independently of mass, the ratios $\tau_2/\tau_1\approx 3.3$ (compared to ≈ 0.9 for linear chains) and $\tau_3/\tau_1\approx 8$ (compared to ≈ 3). This means that, normalizing by the motion of a monomer in the laboratory frame, both the center-of-mass motion and that of monomers in the center-of-mass frame take longer to reach their long-time asymptotic limits than is the case for linear chains.

We now discuss the *probability distribution* $P(x)$ for the mean-square center-of-mass displacement $x=[\mathbf{R}_{\text{c.m.}}(t)-\mathbf{R}_{\text{c.m.}}(0)]^2$. In linear chain systems, all chains behave roughly alike and, on the time scale of motion over one or more gyration radii, the distribution of $\mathbf{R}_{\text{c.m.}}$ is essentially Gaussian. This would lead to $P(x)\propto g_3(t)^{-3/2}x^{-1/2}\exp[-3x/2g_3(t)]$. For rings, another scenario is possible, in which at a given time a small number of rings are relatively ''unentangled'' (for example, with wormlike configurations), as discussed by Klein [11], while others form entangled clusters that can scarcely move. This would yield, in the crudest picture, a bimodal distribution for $P(x)$ at times shorter than the lifetime of a cluster. This possibility is apparently ruled out by the distributions $P(x)$ we obtained, such as, for instance, in Fig. 7 for a melt of rings of mass $N=256$. The distribution for times ranging from much smaller than the relaxation time $\tau_{ee}=1.6\times 10^6$ Monte Carlo steps up to times much larger could be superimposed on one single master curve, which shows precisely the form expected for Gaussian scaling as considered above.

From the mean-square displacement of the center of mass $g_3(t)$ one obtains the diffusion coefficients D_N as shown in Fig. 8 for isolated rings and in Fig. 9 for rings at a volume fraction $\Phi=0.5$. For *isolated* rings in athermal conditions, the diffusion constants obey $D_N\approx 0.034/N$; these are virtually identical to their linear counterparts (Fig. 8), as one expects from an essentially Rouse dynamics in this limit (hydrodynamic forces are of course excluded in our model). The situation is somewhat different for the diffusion constants D_N obtained for rings in the melt. The first striking point is that the rings diffuse *faster* than linear chains of same mass and density. This confirms the trend found experimentally in zero-shear viscosities for PS and PB melts of rings [8].

Second, for rings, there is no sign of curvature on the log plot, which is consistent with the idea that the entanglement mass for rings is larger than for linear chains. In fact, the diffusion constant of linear chains, also shown in Fig. 9, has previously been interpreted in terms of a crossover from true Rouse behavior for small N (which would appear as a plateau on this representation) to a new, entangled regime, with the crossover effects first appearing for $100\leqslant N\leqslant 200$. For linear chains (but not rings) this crossover behavior was much more clearly seen in g_1 and g_3. Looking at the center-of-mass diffusion data alone, however, there is no sign of a small-N plateau and no firm evidence of a crossover to a new regime of entangled behavior, even in the linear chain case. This suggests that other interpretations might also be worth investigating.

If one assumes that, within the range of masses studied, both linear chains and rings follow *a single* power-law behavior, then one finds, respectively, $D\sim N^{-1.5}$ and $D\sim N^{-1.2}$ for the two cases [35]. Remarkably, therefore, in each case that the diffusion constant varies inversely with the mass of the ''correlation hole'' of surrounding chains, $D_N\propto 1/R_g^3$. This suggests a mental picture in which the center-of-mass mobility of any given chain is governed by having to ''drag'' the contents of the correlation hole along with it. Although this picture should clearly break down for long linear chains (where a more conventional reptation picture

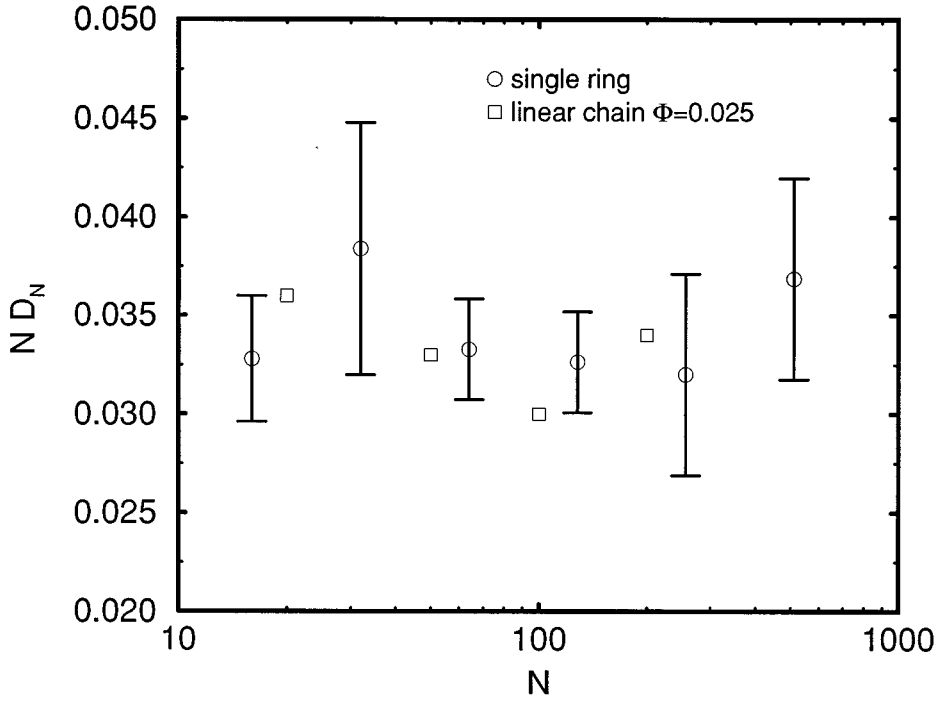

FIG. 8. Diffusion coefficient ND_N versus mass N for isolated rings (circles) and linear chains (squares).

becomes appropriate), it could provide some insight into the behavior at intermediate N. For rings, this ''intermediate'' regime appears to be more strongly developed. If one compares rings and linear chains at equal mean-square gyration radius, then the rings have slightly smaller diffusion constants than linear chains. Assuming that any increase in the entanglement length of rings is due to partial collapse, this is consistent with the experimental fact that the viscosities of ring melts, compared with linear chains at an equal number of entanglements, have slightly higher viscosities.

Master curves for some further correlation functions are presented in Fig. 10. The correlation function $C_{ee}(t)$ is analogous to the end-end vector correlation function usually used for linear chains [9]. It describes the decay of the diameter vector $\langle \mathbf{R}_e(t) \cdot \mathbf{R}_e(0) \rangle$ between two monomers of a ring separated by $N/2$ monomers. The relaxation time τ_{ee}, used to scale the time axis in the various plots discussed already, is defined as the time at which this correlation function has decayed by a factor $1/e$. Note that this correlation function shows a near-exponential decay.

This contrasts with the second correlation function $C_n(t)$, which measures the decay in the mean number of chains, ''touching'' (in the sense defined above) a given reference chain at time zero, that are still touching it (or touching it again) at time t. From this quantity an asymptotic plateau value (arising from the finite size of the simulation

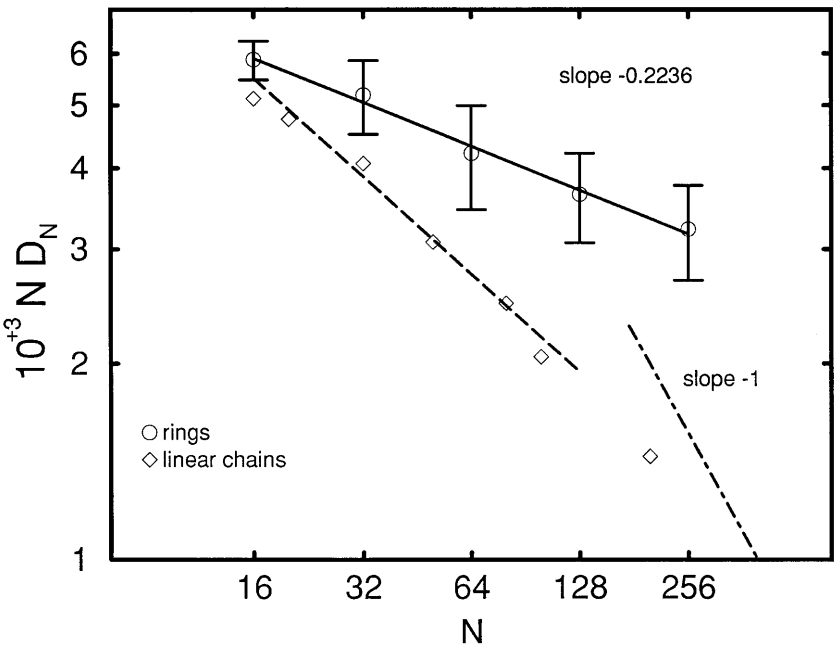

FIG. 9. Diffusion constant of rings (circles) and linear polymer (squares) as a function of the mass N. The diffusion constant of rings varies effectively as $ND_N \propto N^{-0.22}$ (solid line). Neglecting any curvature of the data points, the diffusion constants of linear chains are shown (dashed line) to vary as $ND_N \propto N^{0.5}$. This is compared to the reptation prediction for linear chains (dash-dotted line).

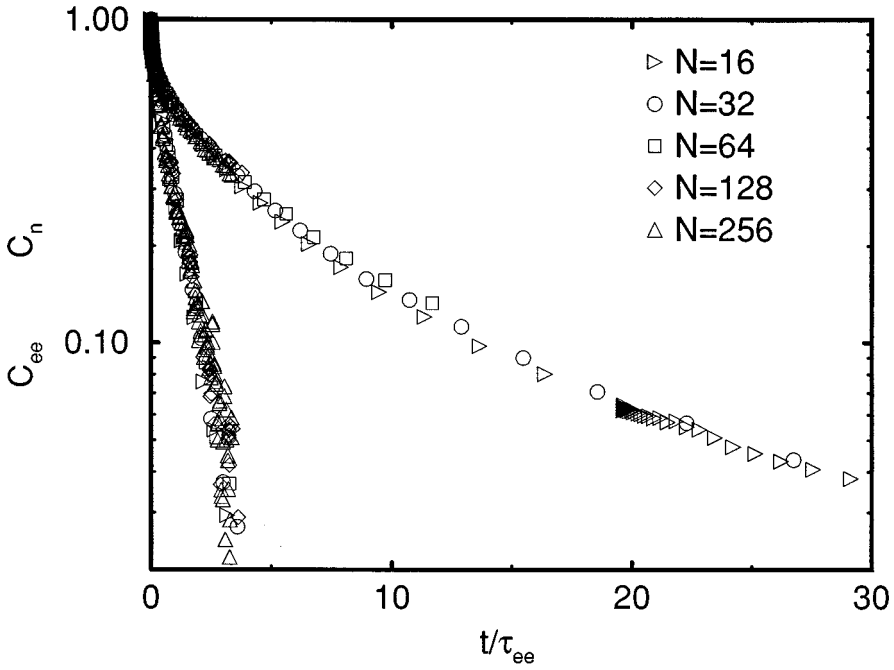

FIG. 10. While the correlation function of the diameter vector $C_{ee}(t)$ (data on the left-hand side of the figure) drops off exponentially, the correlation function $C_n(t)$ measuring the mean number of chains touching a given reference chain decays much more softly with a power law. Data points for various masses superimpose when plotted versus the reduced time t/τ_{ee}.

cell) is subtracted so that the correlation function vanishes at long time; we normalize to $C_n(0)=1$. This $C_n(t)$ apparently decays with a power law (Fig. 10). This correlation function $C_n(t)$ was defined in an attempt to monitor any possible clustering of entangled rings (leading to a fraction of slow-moving material) by detecting possible long-lived contacts between rings that might arise from threading of one ring by another. Although the number of contacting rings remains large for times much longer than the measured diffusive relaxation times, there is nothing like a plateau; the power-law decay of C_n apparently scales with τ_{ee}, so there is no new time scale due to clustering [37]. It seems that the threading probability is not large enough to form large clusters whose percolation (for example) could lead to new dynamical phenomena.

In Fig. 11 we compare the relaxation times τ_{ee} as defined from the decay of the diameter correlation function $C_{ee}(t)$ (and used above for the scaling of the time axis) with the quantity $\langle R_g^2\rangle/D$, which also defines a characteristic time. To a good accuracy, these are proportional, but the latter is larger by a factor of about 10. The scaling of the relaxation time, by either definition, follows approximately an N^2 law (as do the times τ_1, τ_2, and τ_3 we obtained from the mean-square displacements), as predicted from the simple Rouse

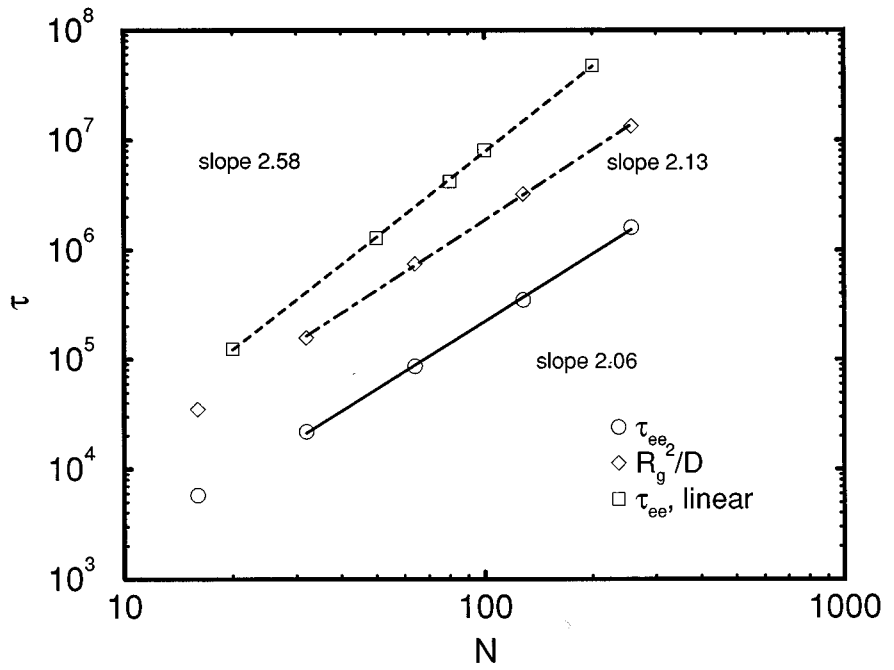

FIG. 11. Reorientation relaxation time τ_{ee} for rings (circles) and linear polymers (squares) obtained from $C_{ee}(t)$ versus polymer mass N. The solid line indicates the exponent 2.06 found for the collapsed molten rings. This value is also confirmed (dash-dotted line) by the relaxation time R_g^2/D_N for rings (diamonds). The relaxation times of linear chains can be fitted by a power law with exponent 2.58, as indicated by the dashed line.

model for Gaussian chains or rings. However, we believe that this is fortuitous, the diffusion constant being the more fundamental quantity; indeed, true Rouse motion for partially collapsed objects (as we know the rings to be) would give a higher power. For comparison, the relaxation time obtained from the diffusion coefficient via R_g^2/D_N for linear chains is also plotted. In the range of N studied, this follows an $N^{2.6}$ power law. (The linear chain values are taken out of Ref. [18] and some data for short chains are added.)

V. CONCLUSION

In this article we have demonstrated, using the bond-fluctuation model, various pronounced effects of topological constraints on the static and dynamic properties of rings. While the size of isolated rings scale as their linear counterparts, molten rings are quite compact objects characterized by an exponent $\nu = 0.39 \pm 0.03$ for the chain size R. This is consistent with a crude Flory-like argument [15] suggesting that one degree of freedom is lost for every nonconcatenation constraint.

Experimentally, melt of rings seem to show dynamical behavior very similar to linear chains, at least for the masses of rings usually studied [8]. The same seems to be true in our computational study, which is of course limited to relatively modest masses, though ones for which, in linear chains, the onset of entanglements would clearly be detectable. We see no sign of a similar effect for rings, suggesting a larger effective entanglement length in the rings case. Indeed, in our simulation (which ignores hydrodynamics but respects the topological constraints) conformational relaxation of the rings is well described by a dynamical scaling involving a single characteristic time scale τ_{ee} for each chain, whereas an entanglement crossover would introduce a second time scale. Nonetheless, the motion is not that of a simple Rouse model (chains moving independently subject to local friction and uncorrelated noise): interchain forces are manifest in the reduced effective exponent for the center-of-mass motion at short time scales or, equivalently, in an increase in the exponent for the dependence of the single-chain relaxation time τ_{ee} on chain length. This increase, fortuitously, approximately restores the exponent to the value 2 predicted by a simple Rouse model for Gaussian rings, despite the fact that our rings are partially collapsed.

The breakdown of a true Rouselike dynamics [which would give $g_3(t) \sim t$] for molten chains is not completely unexpected, since the Rouse model describes only one chain or ring in isolation. What is remarkable from the simulation is that, for the range of masses (of both rings and linear chains) studied so far by BFM, the slowing of the center-of-mass motion is consistent with a picture in which each chain or ring has to drag with it the neighbors in its correlation hole against the resistance of local frictional forces [$D(N) \sim R_g(N)^{-3}$]. This very simple picture may have something to offer for understanding the diffusion of molten linear polymers in what is classically viewed as the crossover region between entangled and unentangled motion, although further work is required to check whether the same relation holds over a range of volume fractions. Note that the diffusion constants and relaxation times for linear chains obtained with the BFM agree perfectly with simulations obtained with molecular dynamics by Kremer and Grest [18] and experimental values of Richter *et al.* by RNA [40]; these were always analyzed previously in terms of a crossover, although such data do not show true Rouse behavior even for small N (neither does the experimental data unless corrections are made for the dependence of the effective segmental mobility on chain length [41]).

Likewise for rings one has to choose whether to assume a crossover or fit an intermediate power law to the data. The crossover interpretation is rather forced for rings, since for the ring sizes studied here, the intermediate (apparently power-law) behavior shows no sign of breaking down at either the small or large mass end of the range. Since the nature of entanglements in ring systems remains to be clarified, it is possible that this behavior could extend to quite high masses (or even, in principle, be the true limiting result for high N). Certainly, if an entanglement crossover is present for rings we can say that it is at substantially higher masses than for linear chains of the same type. In the range of N studied, there is in particular no evidence for a crossover to a regime in which the rings have exponentially long relaxation times. Such behavior would anyway be surprising since even rings in a fixed network show an algebraic dependence of the diffusion constant on mass [15,42]. In molten linear chains, it is known that reptation cannot be the only mode of relaxation (the prefactors predicted from the reptation picture for the diffusion coefficient and for the viscosity systematically underestimate the relaxation), so there are probably enough alternative modes of motion to allow relaxation of molten rings on an algebraic time scale even in the limit of high masses. A full investigation of that limit must of course await further increases of computer power, especially since, as emphasized above, any crossover to the entangled regime occurs for substantially higher masses than in the case of linear chains.

ACKNOWLEDGMENTS

M.M. thanks K. Binder, A. Bruce, W. Paul, and S. Pawley for stimulating discussions; W. Oed for help in porting the program to the CRAY T3D supercomputer; EPFL and EPCC for generous access to their CRAY T3D supercomputer; and the TRACS program for financial support and DFG for Grant No. Bi 314/3-3. J.W. thanks M. S. Turner and W. Paul for stimulating discussions.

[1] K. Dogson and J. Higgins, in *Cyclic Polymers*, edited by J. A. Semlyen (Elsevier, London, 1986).

[2] J. Roovers and P. M. Toprowski, Macromolecules **16**, 843 (1983); J. Roovers, J. Polym. Sci. Polym. Phys. Ed. **23**, 1117 (1985).

[3] G. Hadziioannou, Bull. Am. Phys. Soc. **31**, 355 (1986).

[4] J. Roovers, Macromolecules **18**, 1359 (1985).

[5] G. B. McKenna, G. Hadziioannou, P. Lutz, G. Hild, C. Strazielle, C. Straupe, P. Rempp, and A. J. Kovacs, Macromolecules **20**, 498 (1987).

[6] P. J. Mills, J. W. Mayer, E. J. Kramer, G. Hadziioannou, P. Lutz, C. Strazielle, P. Rempp, and A. J. Kovacs, Macromolecules **20**, 513 (1987).
[7] S. F. Tead, E. J. Kramer, G. Hadziioannou, M. Antonietti, H. Sillescu, P. Lutz, and C. Strazielle, Macromolecules **25**, 3942 (1992).
[8] G. B. McKenna, B. J. Hostetter, N. Hadjichristidis, L. J. Fetters, and D. J. Plazek, Macromolecules **22**, 1834 (1989).
[9] M. Doi and S. F. Edwards, *The Theory of Polymer Dynamics* (Clarendon, Oxford, 1986).
[10] T. P. Lodge, N. A. Rotstein, and S. Prager, Adv. Chem. Phys. **79**, 1 (1990).
[11] J. Klein, Macromolecules **19**, 105 (1986).
[12] J. Klein, D. Fletcher, and L. J. Fetters, Nature **304**, 526 (1983); C. R. Bartels, B. Crist, Jr., L. J. Fetters, and W. W. Graessley, Macromolecules **19**, 785 (1986); M. Antonietti and H. Sillescu, *ibid.* **19**, 798 (1986).
[13] If only the data points for the high masses are considered the exponent in the entangled regime is $\alpha_2 \approx 3.5$. If one insists on a Rouse-like behavior ($\alpha_1 = 1$) at low molecular weight as for linear chains, the viscosities are fitted with $\eta_0 = aM + bM^{\alpha_2}$, giving a somewhat higher exponent in the entangled regime of $\alpha_2 \approx 3.8 - 3.9$ [5].
[14] The motion of rings in linear matrices is, on the other hand, slowed down compared to linear chains in linear matrices. This is easy to rationalize in terms of the threading of rings by linear matrix chains [6].
[15] M.E. Cates and J. M. Deutsch, J. Phys. (Paris) **47**, 2121 (1986).
[16] T. Pakula and S. Geyler, Macromolecules **21**, 1665 (1988).
[17] S. Geyler and T. Pakula, Macromol. Chem. Rapid Commun. **9**, 617 (1988).
[18] W. Paul, K. Binder, D. Heermann, and K. Kremer, J. Phys. (France) II **1**, 37 (1991); J. Chem. Phys. **95**, 7726 (1991).
[19] J. Wittmer, W. Paul, and K. Binder, Macromolecules **25**, 7211 (1992).
[20] J. S. Shaffer, J. Chem. Phys. **103**, 761 (1995).
[21] H.-P. Deutsch and K. Binder, J. Chem. Phys. **94**, 2294 (1991); I. Carmesin and K. Kremer, Macromolecules **21**, 2819 (1988).
[22] H.L. Frisch, M. Schulz, and P.R.S. Sharma, Comput. Polym. Sci. **4**, 13 (1994).
[23] T. Pakula, Macromolecules **20**, 679 (1987).
[24] T. Pakula and S. Geyler, Macromolecules **20**, 2909 (1987).
[25] M. Müller, K. Binder, and W. Oed, Sci. Programming (to be published); M. Müller (unpublished).
[26] The exponent ν for isolated rings in two dimensions is also similar to the linear chain result, as shown by several authors [28,29], obtaining $\nu \approx 0.745$; in this case, however, it is not clear that a distinction can be made between the excluded volume and topological interactions.
[27] J. des Cloizeaux and M. L. Metha, J. Phys. (Paris) **40**, 665 (1979).
[28] D. Gersappe and M. Olvera de la Cruz, Phys. Rev. Lett. **70**, 461 (1993).
[29] M. E. Fisher, Physica (Amsterdam) A **38**, 112 (1989).
[30] E. F. Casassa, J. Polym. Sci A **3**, 605 (1965).
[31] Fortunately, the universal function corresponding to the finite-size effect appears to be analytic.
[32] M. G. Brereton and T. A. Vilgis, J. Phys. A **28**, 1149 (1995).
[33] P.-G. de Gennes, *Scaling Concepts in Polymer Physics* (Cornell University Press, Ithaca, 1979).
[34] For comparison, the structure factor for a Gaussian ring is given, e.g., in Ref. [36]. A detailed comparison of molten rings with the Gaussian statistics was made previously in Ref. [16].
[35] Skolnick *et al.* [38] also obtained in their simulation of linear chains at volume fraction $\Phi = 0.5$ a diffusion constant $D_N \propto N^{-3/2}$ and a longest autocorrelation time of $\tau \propto N^{2.5}$ for chains up to 216 monomers on a cubic lattice. For linear chains, this result is close to ours and also close to that of Schweizer's ''renormalized Rouse model'' [39], which is intermediate between classical Rouse and reptation models, predicting $D_N \propto N^{-3/2}$ and $\tau \propto N^{5/2}$.
[36] W. Burchard and M. Schmidt, Polymer **21**, 745 (1980).
[37] The shape of the correlation functions $C_n(t)$ is perhaps not unique to rings. In their simulations Skolnick *et al.* [38] examined for linear chains the survival of long-lived two-chain contacts, which decayed in a multiexponential manner, with a significant population at times greater than the longest relaxation time τ.
[38] A. Kolinski, J. Skolnick, and R. Yaris, J. Chem. Phys. **86**, 1567 (1987); **84**, 1922 (1986); **86**, 7164 (1987); **86**, 7174 (1987).
[39] K. S. Schweizer, J. Chem. Phys. **91**, 5802 (1989); **91**, 5822 (1989); K. S. Schweizer and G. Szamel, *ibid.* **103**, 1934 (1995).
[40] D. Richter, L. Willner, A. Zirkel, B. Farago, L. J. Fetters, and J. S. Huang, Macromolecules **37**, 7437 (1994).
[41] J. D. Ferry, *Viscoelastic Properties of Polymers*, 3rd ed. (Wiley, New York, 1980).
[42] J. Reiter, J. Chem. Phys. **95**, 1290 (1991).